Journal of Applied Polymer Science

Poly(ethylene terephthalate)/poly(ethylene glycol-*co*-1,3/1,4-cyclohexanedimethanol terephthalate)/clay nanocomposites: Effects of biaxial stretching

Jyh-Horng Wu,[1] Ming-Shien Yen,[2] M. C. Kuo,[2] Yuhsin Tsai,[3] Ming-Tsong Leu[1]

[1]Green Energy & Eco-Technology Center, Industrial Technology Research Institute, Tainan, Taiwan

[2]Department of Materials Engineering, Kun Shan University, Tainan, Taiwan

[3]School of Chinese Medicine, China Medical University, Taichung, Taiwan

Correspondence to: M. C. Kuo (E-mail: muchen@mail.ksu.edu.tw) and Y. Tsai (E-mail: yhtsai@mail.cmu.edu.tw)

ABSTRACT: In this study, we fabricated poly(ethylene terephthalate) (PET)/clay, PET/poly(ethylene glycol-*co*-1,3/1,4-cyclohexanedimethanol terephthalate) (PETG), and PET/PETG/clay nanocomposite plates and biaxially stretched them into films by using a biaxial film stretching machine. The tensile properties, cold crystallization behavior, optical properties, and gas and water vapor barrier properties of the resulting films were estimated. The biaxial stretching process improved the dispersion of clay platelets in both the PETG and PET/PETG matrices, increased the aspect ratio of the platelets, and made the platelets more oriented. Thus, the tensile, optical, and gas-barrier properties of the composite films were greatly enhanced. Moreover, strain-induced crystallization occurred in the PET/PETG blend and in the amorphous PETG matrix. © 2015 Wiley Periodicals, Inc. J. Appl. Polym. Sci. **2015**, *132*, 42207.

KEYWORDS: blends; clay; composites; polyesters

Received 22 September 2015; accepted 13 March 2015

DOI: 10.1002/app.42207

INTRODUCTION

Poly(ethylene terephthalate) (PET) is a commercially important engineering polymer with good thermal and mechanical properties, low permeability, and good chemical resistance.[1–4] It is widely used in textiles, bottle containers, food packaging, automobiles, and blood vessel tissue engineering.[4–7] As proposed, the inclusion of organoclay into the PET matrix can substantially reduce the oxygen transmission rate (OTR) and water vapor transmission rate (WVTR) of the resulting PET/clay nanocomposites.[6] However, PET/clay nanocomposites are generally opaque due to high crystallinity arisen by the inclusion of clay, and under this condition the nanocomposites can no longer be used in food and beverage packaging. Poly(ethylene glycol-*co*−1,3/1,4-cyclohexanedimethanol terephthalate) (PETG) is an amorphous thermoplastic of the commercial PET family, with physical properties similar to PET.[8–10] Papadopoulou and Kalfoglou reported that the PET/PETG blend has a single endothermic peak in both T_g (93.3°C) and T_m (235.0°C) at a mixing ratio of 50/50 under the second heating run, indicating that this blend has good compatibility.[11] In our previous study, we demonstrated that the amorphous nature of PETG is unaffected by including clay.[5] We fabricated PET/PETG/clay nanocomposites and investigated the mechanical and barrier properties, optical transparency, and crystallization kinetics of these composites.[5,6]

Including 6 phr (parts per hundred of rubber or resin) of organoclay into a PET matrix increases the crystallinity of PET/clay by approximately 7%, compared with that of including untreated PET. However, the half crystallization times for PET and PET/clay are 4.36 and 2.10 min, respectively, when these specimens are isothermally crystallized at 215°C. By contrast, including PETG into the crystalline PET would dilute the crystallinity of PET/clay composites.[4] Incorporation clay into PET diminishes the crystallinity of PET/clay composites. Incorporating clay into the PET matrix certainly increases the barrier properties but also considerably decreases optical transparency. Alternatively, PET/PETG/clay can improve its gas-barrier properties and simultaneously maintain its gas-barrier properties and simultaneously maintained its transparency.[6]

As reported, the biaxial stretching process easily enhances the physical properties of PET nanocomposites. The process also increases the barrier properties, crystallinity, and thermal stability of the nanocomposites.[4,12–14] Biaxial stretching also improve the physical and thermal properties of polymers other than PET, such as polypropylene (PP), polystyrene (PS), and the biodegradable poly(lactic acid) (PLA). We previously fabricated PLA films and investigated the effects of biaxial stretching on thermal properties, crystallinity, shrinkage, and mechanical properties on them. Our study showed that PLA shrinkage

Table I. Effect of Stretch Ratio on the Tensile Properties of the Biaxially Stretched PET/Clay, PETG/Clay, and PET/PETG/Clay Nanocomposites

Materials	Stretching ratio	Modulus (MPa)	Tensile strength (MPa)	Elongation (%)
PET/clay (100/6) [a]	Unstretched	2770	32	1.1
	1	3029	54	2.0
	2	3779	61	28.0
	3	3994	72	30.2
PETG/clay (100/6) [a]	Unstretched	2600	21	1.2
	1	2836	38	1.9
	2	3458	57	31.0
	3	3656	65	39.0
PET/PETG/clay (50/50/6) [a]	Unstretched	2646	28	0.9
	1	2997	52	2.4
	2	3485	65	32.0
	3	3858	68	34.1

[a] clay was mixed with different aspect ratio of Closite 15A and MPGN in 1 : 1 weight ratio.

decreased proportionally to the stretch rate and inversely proportionally to the stretching temperature. Furthermore, the mechanical properties of the PLA films increased considerably after biaxial stretching.[15]

Because of the improved mechanical and barrier properties compared with those of PLA films, and the optical transmittance of the PET/clay, PETG/clay, and PET/PETG/clay film products, investigating the effects of biaxial stretching on these properties proved compelling. The biaxially stretched films of PET/clay, PETG/clay, and PET/PETG/clay were fabricated, and the mechanical, optical, and barrier properties were determined to estimate their performance.

EXPERIMENTAL

Materials

The PET polymer (SHINPET 5015W) was kindly supplied by Shinkong Synthetic Fibers Co., Taiwan. PETG was prepared by two-stage melt-polycondensation (esterification and polycondensation) in an autoclave reactor. The molar ratio of ethylene glycol (EG)/1,3/1,4-cyclohexanedimethanol (1,3/1,4-CHDM) was 70/30. The details of the synthesis can be found in our previous study.[16] Cloisite 15A (aspect ratio: 75–100, quat concentration: 125 mequic/100g, X-ray d_{001}: 3.14 nm, density: 1.66 g/cm^3) was purchased from Southern Clay Products Inc. Cloisite 15A is a natural montmorillonite modified with dimethyl dihydrogenated tallow quaternary ammonium chloride. PGN (aspect ratio: 300–500, quat concentration: 120 mequic/100g, density: 2.60 g/cm^3) was purchased from NANOCOR Co. Modified PGN (MPGN) is a natural montmorillonite modified with dimethyl distearylammonium chloride (X-ray d_{001}: 3.41 nm). It is worth to claim that the organoclay used in this study was obtained by mixing Cloisite 15A with MPGN in 1 : 1 weight ratio.

Preparation of the Biaxially Stretched Films

The PET/clay, PETG/clay, and PET/PETG/clay nanocomposites were carefully dried and then extruded at temperatures of 230–260°C by a twin-screw (Werner and Pflederer, Model-ZSK 26 MEGA compounder) using a screw speed of 500 rpm to form flat sheets 20 cm wide and 0.53 mm thick. From the sheets, 117 mm × 117 mm plates were cut. The plates were inserted into a biaxial film stretch machine (Bruckner, KARO IV) to prepare the biaxially stretched films at 103°C. The biaxial stretch ratios were 1–3 at stretch rate of 100%/sec.

Tensile Properties

Tensile strength, tensile modulus and elongation at break were measured by a Universal Tensile Tester with a cross-head speed of 25 mm min^{-1} in compliance with the specifications of ASTM D638.

Optical Properties

Total light permeation coefficient (T) were measured by a Haze/Turbidimeter (Nippon Denshoku Industries, Japan, model No. NDH 2000) according to the ISO 14782 methods.

Differential Scanning Calorimetry Analysis

Differential scanning calorimetry analysis (DSC) was performed using a TA apparatus (model No. Q2000). The weights of specimens used in the DSC scan are 4–5 mg. The test was first heated from 30 to 300°C at a heating rate of 5°C min^{-1} under nitrogen atmosphere.

X-ray Measurements

X-ray diffraction (XRD) measurements were conducted on a Rigaku D/Max RC X-ray diffractometer using CuK_α radiation ($\lambda = 1.5418$ A) at 40 kV and 100 mA with a scanning rate of 2° min^{-1}.

Transmission Electron Microscopic Analysis

Transmission electron micrographs (TEM) of PET/clay, PETG/clay, and PET/PETG/clay nanocomposites were taken in a HITACHI H7500 TEM with an acceleration voltage of 120 kV. The specimens were prepared using an ultrathin microtome. Thin sections of about 100 nm were cut with a diamond knife at 30°C.

Oxygen and Water Vapor Transmission Measurement

The transmission rates (oxygen and water vapor) were measured by Mocon OX-TRAN Model 2/61 universal apparatus.

OTR was according to ASTM D 3985, 40°C and 0% relative humidity (RH). WVTR was according to ASTM F 1249, 40°C and 100% RH. The specimen test area and thickness were 5 cm^2 and 0.6 mm, respectively, for all specimens.

POM Observations

A Nikon Optiphot-Pol universal stage polarizing optical microscope (Tokyo, Japan) was used to observe the spherulite morphologies of the PET/clay, PETG/clay, and PET/PETG/clay under isothermal crystallization. A thin piece of sample was sandwiched between two glass coverslips and placed on a digital hot-stage under nitrogen atmosphere. The hot-stage was rapidly heated to 300°C and held for 3 min to erase the thermal history of specimens. Then, the PET/clay, PETG/clay, and PET/PETG/clay melts were quenched to the predetermined crystallization temperatures and kept at these temperatures for observations.

RESULTS AND DISCUSSION

Tensile Properties

To estimate the performance of the PET/clay, PETG/clay, and PET/PETG/clay composites the tensile properties of the biaxially stretched films prepared using these composites were determined (Table I). The content of organoclay in all three of the nanocomposites was 6 phr, and the biaxial stretch ratios were 1–3 at a stretch rate of 100%/s at 103°C. The results in Table I show that both the modulus and tensile strength of the PET/clay, PETG/clay, and PET/PETG/clay nanocomposites increase with increasing stretch ratios. We believe that a higher stretch ratio brings the polymer molecules into tight proximity and causes random molecules to become more uniformly oriented.

In our previous study, the stress and strain values of PLA films increased considerably as a function of the stretch ratio.[15] Zhang *et al.* studied the biaxially stretched PS and proposed that the tensile modulus, stress, and elongation at break of the stretched PS specimens increased with increasing stretch ratio along both machine and transverse directions. The tensile stress increased from 20 MPa to 80 MPa (400% increase), and the highest elongation at break increased from less than 1% to 4.5% (450% increase) as the stretch ratio ranged from 1 to 6.[17] In our present study, the stress increments for the PET/clay, PETG/clay, and PET/PETG/clay at the stretch ratio 3.0 are 125%, 210%, and 143%, respectively, compared to the unstretched counterparts. As shown in Table I, the values of elongation at break increase significantly and greatly from 1.1% to 30.2% for PET/clay at the stretch ratio ranging from null to 3, and those are 1.2% to 39.0% and 0.9% to 34.1% for PETG/clay and PET/PETG/clay, respectively.

Rajeev *et al.* investigated the effect of equistretching on the exfoliation of nanoclays in a PET matrix, proposing that stretching not only improves the exfoliation as the concentration of thinner tactoids in the matrix increases but also causes an increase in the concentration of longer tactoids and tactoids with higher aspect ratios. They postulated that the slippage of the platelets during stretching might be responsible for such increased exfoliation.[18] In the present study, TEM showed that the tactoids in the PET/PETG blend have higher aspect ratios and orientation after biaxial stretching, as shown in Figure 1.

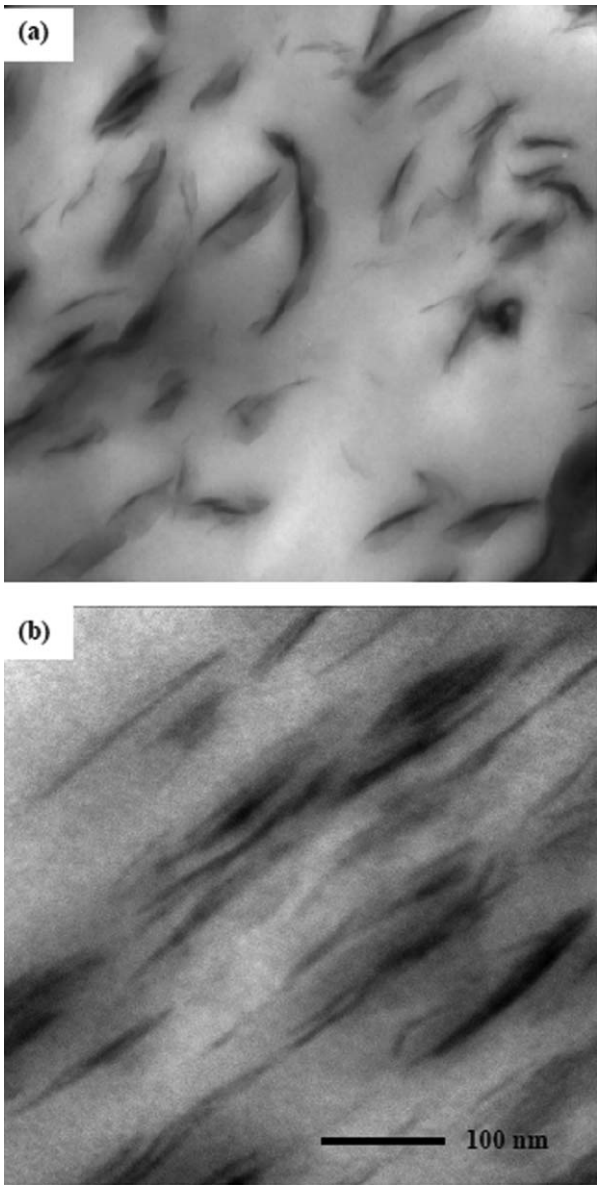

Figure 1. TEM micrographs of (a) unstretched and (b) biaxially stretched (3×) PET/PETG/clay nanocomposites.

Moreover, the XRD patterns on the unstretched and biaxially stretched PET/clay, PETG/clay, and PET/PETG/clay composites revealed increased concentrations with thinner and longer tactoids in the PET and PET/PETG matrices, as shown in Figure 2. The diffraction peaks at $2\theta = 2.370^{o} \sim 2.555^{o}$ are the characteristic diffraction of the (001) plane of Closite 15A clay. Apparently, the diffraction intensities increased with increasing stretching ratios, indicating that the slippage occurred within the platelets of organoclay during the biaxially stretching process, and that this slippage may induce the further exfoliation of the organoclay. Our result is consistent with that of PET/clay proposed by Rajeev *et al.* Because of the increases in the thinner and higher aspect-ratio tactoids in the PET and PET/PETG matrices, the values of elongation at break for the stretched PET/

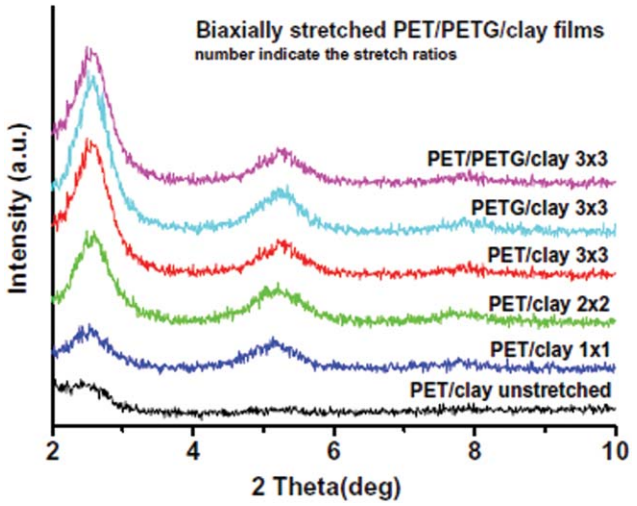

Figure 2. XRD patterns of biaxially stretched PET/clay, PETG/clay, and PET/PETG/clay nanocomposites. [Color figure can be viewed in the online issue, which is available at wileyonlinelibrary.com.]

clay, PETG/clay, and PET/PETG/clay showed considerable improvement.

Regarding the modulus values in Table I, we found that the increments of the PET/clay composite were 9.4%, 36.4%, and 44.1% for the 1 × 1, 2 × 2, and 3 × 3 biaxial stretch ratios, respectively, compared with those of the unstretched counterpart. Furthermore, the increments of the PETG/clay and PET/PETG/clay composites were 9.1%, 33.0%, and 40.6%, and 13.3%, 31.7%, and 45.8%, respectively. We tentatively propose that the tensile modulus of the stretched PET/clay, PETG/clay, and PET/PETG/clay films increases linearly with the stretch ratio. We believe that the higher the stretch ratio is, the more tightly closed the polymer molecules become, which in turn increases the stiffness of the molecules.

Regarding the tensile strength of the PET/clay, PETG/clay, and PET/PETG/clay films, we found that the values of tensile strength for these composites were more sensitive to the stretch ratio than to the modulus increments. The tensile strength increments of the PET/clay composite were 69%, 91%, and 125%; those of the PETG/clay composite were 81%, 171%, and 210%; and those of the PET/PETG/clay composite were 86%, 132%, and 143%, for the 1 × 1, 2 × 2, and 3 × 3 biaxial stretch ratios, respectively.

Cold Crystallization Behavior

The three studied nanocomposites were heated from 30° to 300°C at a heating rate of 5°C min^{-1} in a nitrogen atmosphere by using a DSC (TA Q2000) instrument. Figure 3 shows the cold crystallization DSC traces of these nanocomposites with 1 × 1, 2 × 2, and 3 × 3 biaxial stretch ratios. The glass transition temperature, T_g (first heating), melting temperature, T_m (first heating), and cold crystallization temperature, T_{cc} (first heating) were estimated based on the maximum of the peaks. The degree of crystallinity, X_c, was evaluated using the following equation:

$$X_c = \frac{\Delta H_m - \Delta H_{cc}}{(1-f_c)(\Delta H_{m-\text{crystal}})} \times 100 \quad (1)$$

ΔH_m and ΔH_{cc} are the melting and cold crystallization enthalpies, respectively, and ϕ_c is the weight fraction of filler. A wholly crystallized PET $\Delta H_{m-\text{crystal}}$ is assumed to be equal to 119.8 J/g.[19] As shown in Table II, the crystallinities of the PET/clay and PET/PETG/clay nanocomposites are shown to have increased with increasing stretch ratios. For specimens with a stretch ratio

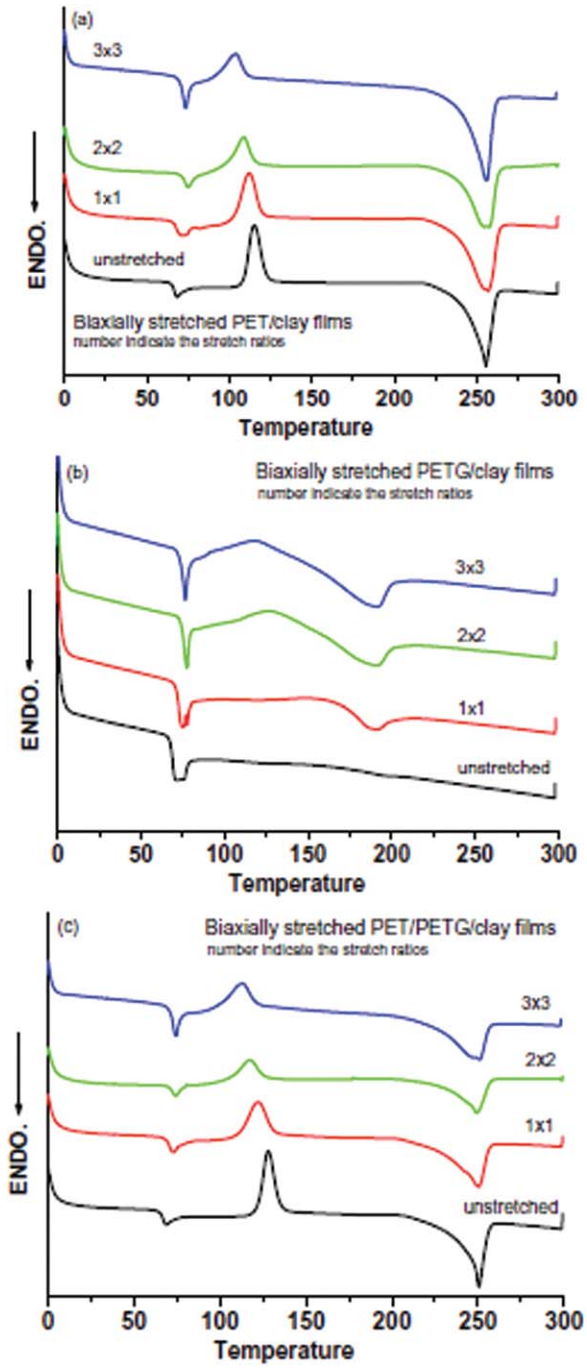

Figure 3. DSC traces of the (a) PET/clay, (b) PETG/clay and (c) PET/PETG/clay at various stretched ratios. [Color figure can be viewed in the online issue, which is available at wileyonlinelibrary.com.]

Table II. Cold Crystallization Parameters of the Biaxially Stretched PET/Clay, PETG/Clay, and PET/PETG/Clay Nanocomposites

Materials	Stretching ratio	Crystal sp heat (J/g)	Melt sp heat (J/g)	X_c (%)	T_g (°C)	T_m (°C)
PET/clay (100/6)						
	Unstretched	29.59	63.45	29.96	67	256
	1	21.76	61.80	35.43	68	256
	2	15.89	58.26	37.49	74	256
	3	14.60	60.15	40.31	73	257
PETG/clay (100/6)	Unstretched	-	-	-	69	-
	1	2.03	5.92	3.44	73	189
	2	8.09	17.02	7.90	73	191
	3	10.05	20.67	9.40	75	190
PET/PETG/clay (50/50/6)	Unstretched	28.15	48.44	17.95	67	250
	1	23.92	47.90	21.22	71	250
	2	16.92	42.88	22.97	73	250
	3	16.11	42.58	23.42	73	251

of 3 × 3, the crystallinity of PET/clay increased from 29.96% to 40.31% (increment 10.35%) for the unstretched specimen, and that of the PET/PETG/clay increased from 17.95% to 23.42% (increment 5.47%) for the unstretched specimen. As stated previously, the stretching process makes the tactoids smaller and increases the aspect ratio.[18] Based on this finding, the specific area of the organoclay becomes larger during the stretching process, thereby increasing the possibility of heterogeneous nucleation. The strain-induced crystallization might increase the crystallinities of the PET/clay and PET/PETG/clay composites. Ajji *et al.* found that drawing on amorphous PET film at 80°C increases the orientation and crystallinity of the amorphous PET.[20] However, including amorphous PETG considerably retards the crystallization process. The crystallinity of the PET/PETG/clay composite is much lower than that of PET/clay. In Figure 4(a), the characteristic Maltese-cross pattern of the PET spherulites is obvious and widespread in the PET/clay composite, but this pattern is absent from the PET/PETG/clay composite [Figure 4(b)] because of the inclusion of amorphous PETG. In our previous study on the isothermal crystallization behavior of the PET/PETG/clay nanocomposite, we proposed that including amorphous PETG substantially decreases the crystallinity of the crystallizable PET units of PET. Morphologically, including amorphous PETG drives the crystallites of the PET matrix from a spherulite to the two-dimensional and disc-like morphology of the PET/PETG blended matrix.[5]

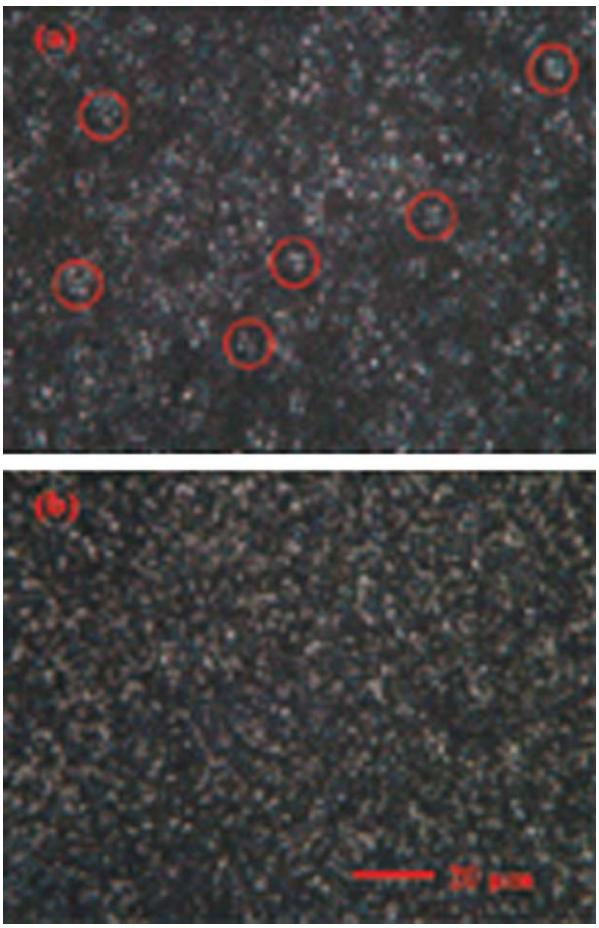

Figure 4. The spherulite morphologies of (a) PET/clay and (b) PET/PETG/clay at 225 and 205°C, respectively, for 60 s. The circled in the pictures are the spherulite morphology of PET polymer. [Color figure can be viewed in the online issue, which is available at wileyonlinelibrary.com.]

Notably, strain-induced crystallization occurred in the amorphous PETG/clay nanocomposite, as shown in Figure 3(b) and Table II. The crystallinity of the unstretched PETG/clay was nil, but the crystallinities of the 1 × 1, 2 × 2, 3 × 3 specimens were 3.44%, 7.90%, and 9.40%, respectively. In Figure 3(b), the cold crystallization DSC traces of the biaxially stretched PETG/clay specimens appear to exhibit weakly exothermic cold-crystallization peaks. The DSC baseline for the unstretched PETG/clay specimen [Figure 3(b)] shows an unperturbed trace. However, the baselines for the biaxially stretched PETG/clay specimens exhibit the perturbations between 95°C and 195°C, consisting of weak exothermic and apparent endothermic peaks. Kattan *et al.* also observed strain-induced crystallization in uniaxially drawn PETG plates, and found that the crystallinity of the PETG copolymer with a uniaxially drawn ratio of 6.4

Table III. Effect of Stretch Ratio on the Optical Properties of the Biaxially Stretched PET/Clay, PETG/Clay, and PET/PETG/Clay Nanocomposites

Materials	Stretching ratio	Thickness (mm)	Total light transmittance (%)	Haze (%)
PET	Unstretched	0.53	79.3	51.5
	1	0.15	88.2	47.2
	2	0.07	88.8	44.3
	3	0.05	89.6	43.6
PETG	Unstretched	0.53	90.3	43.1
	1	0.15	90.1	23.2
	2	0.07	90.2	22.9
	3	0.04	90.3	22.1
PET/PETG	Unstretched	0.53	85.4	55.1
	1	0.15	87.6	47.2
	2	0.06	88.2	39.3
	3	0.03	88.8	31.2
PET/clay (100/6)	Unstretched	0.53	70.7	65.0
	1	0.15	87.3	63.2
	2	0.06	87.4	59.1
	3	0.04	87.5	48.8
PETG/clay (100/6)	Unstretched	0.53	77.3	51.3
	1	0.15	84.4	32.3
	2	0.08	86.3	31.7
	3	0.03	87.1	30.5
PET/PETG/clay (50/50/6)	Unstretched	0.53	76.7	63.9
	1	0.15	86.4	58.2
	2	0.05	88.6	50.1
	3	0.02	89.7	41.3

reached as high as 18%.[21] The findings of the present study on the strain-induced crystallization of PETG/clay are consistent with those of Kattan *et al.*

As shown in Table II, the biaxial stretching process had little effect on the first transition temperatures of the three composite specimens. The melting temperatures for these specimens remained relatively invariant. However, the second transition temperature increased with increasing stretch ratios for all of the PET/clay, PETG/clay, and PET/PETG/clay films. As mentioned, biaxial stretching induced increased concentrations of thinner and longer tactoids in the PET and PET/PETG matrices; this spreading of the hard segment of tactoids might cause the PET/clay, PETG/clay, and PET/PETG/clay nanocomposites to become more rigid than their unstretched counterparts.

Optical Properties

The PET/clay, PETG/clay, and PET/PETG/clay nanocomposites were subjected to biaxial stretching in 1 × 1, 2 × 2, and 3 × 3 ratios. The optical properties of these nanocomposites are listed in Table III. The total light transmittance of the PET/clay composite film with a 1×1 stretch ratio is 87.3%, and that of the unstretched PET/clay film is 70.7%. Increasing the stretch ratio further in PET/clay nanocomposites had little effect on light transmittance.

As stated previously, the stretching process not only improves the exfoliation as the concentration of thinner tactoids in the matrix increases but also causes an increase in the concentration of longer tactoids and tactoids with higher aspect ratios. Rajeev *et al.* found that the concentration of thinner platelets in the thickness range 1–2 nm increased from 10% to 30%, and those in the range 2–3 nm increased from 10% to 25% after equi-stretching at a stretch ratio of 3. By contrast, platelets in the thickness range 10–15 nm for the unstretched sheet were as high as 21% compared with those for the stretched sheet (6%).[18] In the present study, the clay platelets in the unstretched PET/PETG/clay film were largely within the range 20–45 nm, despite half of the platelets being dispersed in the thickness range 20–40 nm after biaxial stretching (3 × 3). However, many platelets are dispersed more thinly and oriented with long aspect ratios compared with those of unstretched PET/PETG/clay film. The stretching process not only makes the films (including PET/clay, PETG/clay, and PET/PETG/clay) thinner, as shown in Table III, but also increases the possibilities of thinner and longer platelets. Consequently, the domain sizes of clay platelets in the PET and PET/PETG matrices become smaller.

The dispersion picture of clay platelets is schematized in Scheme 1. The PET or PETG polymer chain was oriented and aggregated to form the crystallites (circled domains in Scheme 1) after biaxial stretching, and the clay platelets decreased their domain size and oriented towards the machine direction. As shown in Table III, the total light transmittance of the PET/clay,

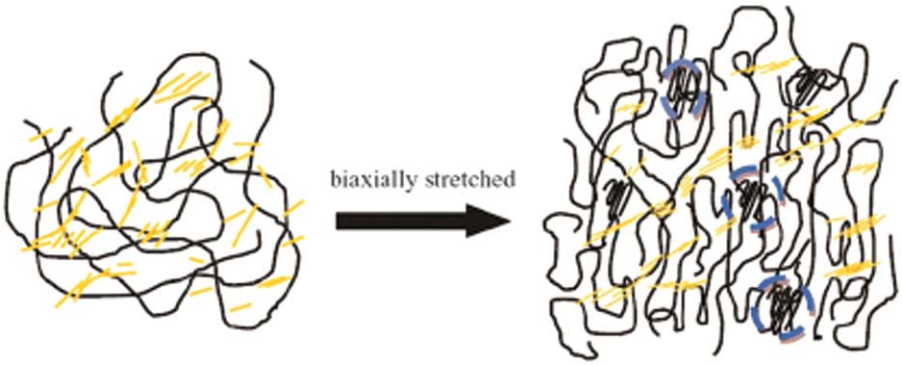

Scheme 1. The schematic diagrams illustrating the transformation of the random coils into the oriented aggregations (circled) of molecular segments due to biaxial stretching. The polymer chains are denoted by the solid lines, and the clay platelets in the polymer matrix are denoted by yellow plates. [Color figure can be viewed in the online issue, which is available at wileyonlinelibrary.com.]

PETG/clay, and PET/PETG/clay nanocomposites increased with increasing biaxial stretch ratios because of the effect of the stretch ratio on the domain sizes, which are considerably smaller than the wavelength of visible light thus causing the clay platelets to become smaller and the nanocomposite films to become thinner. The haze values for the PET/clay nanocomposites also decreased with increasing biaxial stretch ratios because of the smaller domain size of clay platelets in the PET matrix.

Lin *et al.*, used atomic force microscope (AFM) to characterize the roughness of the surfaces of biaxially-oriented polypropylene (BOPP) films, and they proposed that the large-scale roughness surface caused primarily by the spherulites, which may be as large as 200 μm in PP films, and the spherulite boundaries. Surface roughness on the submicron size scale, which may be resulted from the lamellar or fibril structure, did not affect the transparency.[22] They also proposed that the large-scale roughness has a considerable effect on the haze value of the BOPP film. In the present study, the spherulite dimension for the PET/clay film is approximately 5–8 μm, much less than the dimension of PP spherulites. Therefore, we think that the increases of crystallinities in the biaxially stretched PET/clay, PETG/clay, and PET/PETG/clay films should not play the major role on the on values of total light transmittance and haze of the films. The smaller domain size of clay platelets in the PET or PET/PETG matrix and the much thinner films of the stretched specimens should be responsible for the improvements of total light transmittance and haze of the films.

Including amorphous PETG into the crystalline PET increased the total light transmittance of the resulting PET/PETG/clay composite. The value of light transmittance increased with increasing stretch ratios, compared with the PET/clay composite, in which the stretch ratio has little effect on light transmittance. As shown in Table II, including amorphous PETG retards the crystallization process and decreases the crystallinity of the PET polymer, resulting in improved light transmittance in the PET/PETG/clay nanocomposites subjected to a high ratio of biaxial stretching.

Water Vapor and Oxygen Barrier Properties

It was proposed that including nanofillers, particularly for the clay platelets, can improve the gas-barrier properties of the composites against oxygen and water vapor. In our previous study on the barrier properties of the unstretched PET/PETG/clay nanocomposites, we found that the values of the OTR were improved by approximately 38%, 13%, and 28% for the organoclay-filled PET, PETG, and PET/PETG blends, respectively,

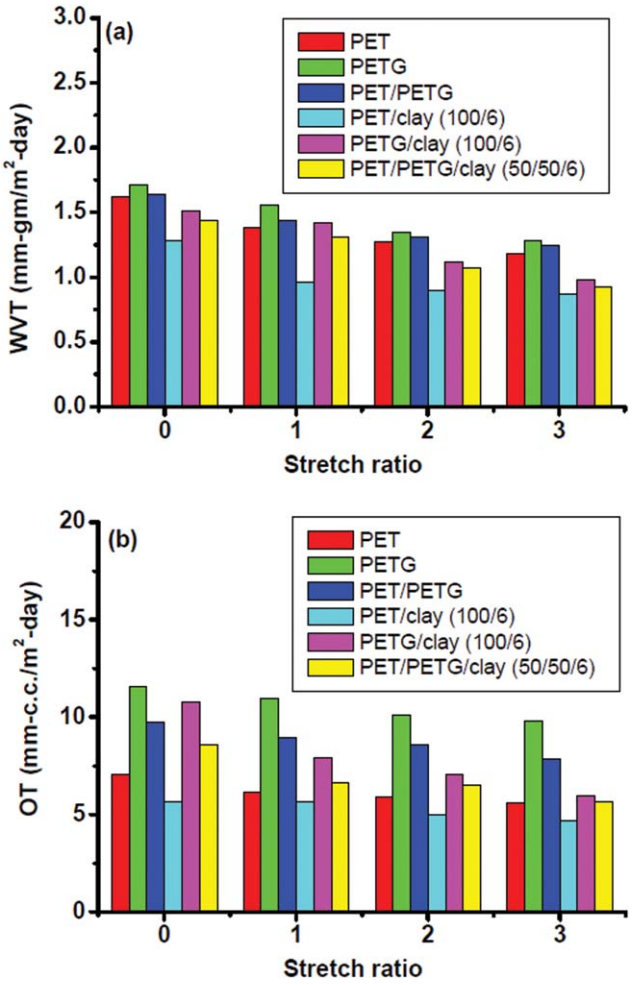

Figure 5. Effect of stretch ratio on (a) WVTR and (b) OTR of the biaxially stretched PET/clay, PETG/clay, and PET/PETG/clay nanocomposites. [Color figure can be viewed in the online issue, which is available at wileyonlinelibrary.com.]

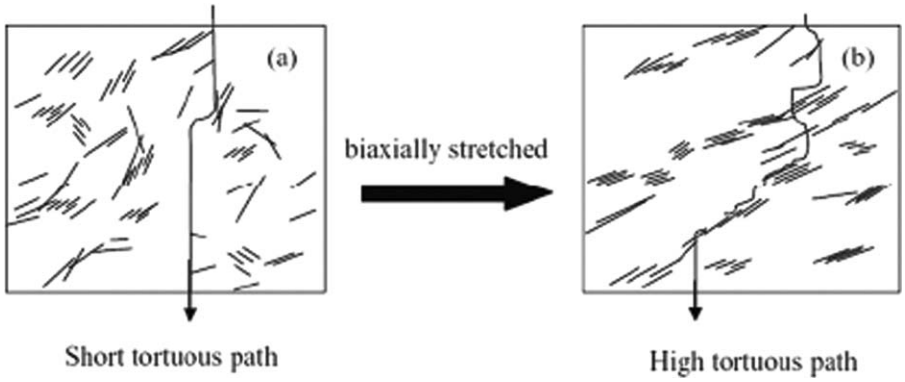

Scheme 2. Schematic representation of gas or water vapor molecules diffusing through the PET/PETG/clay nanocomposite (a) without biaxial stretching and (b) with biaxial stretching.

compared with those of the unfilled counterparts.[6] In our present study, on the biaxial stretching of PET/clay, PETG/clay, and PET/PETG/clay, the stretching process considerably decreased the OTR and water vapor transmission rate (WVTR) values of the specimens, as shown in Figure 5. For the PET/clay composite, the WVTR values were 1.28, 0.96, 0.90, and 0.87 mm-gm/mm^2-day for the stretch ratios of null, 1 × 1, 2 × 2, and 3 × 3, respectively. The biaxial stretch ratio of 3 × 3 improved the WVTR performance of PET/clay composite by approximately 32% compared with that of the unstretched PET/clay. Regarding the PETG/clay and PET/PETG/clay nanocomposites, the biaxial stretch ratio of 3 × 3 also improved their WVTR performance by 35%. The OTR values of the PET/clay, PETG/clay, and PET/PETG/clay nanocomposites also decreased gradually with increasing stretching ratios. For the PET/clay composite, the OTR values were 5.71, 5.66, 4.98, and 4.68 mm-c.c./mm^2-day for the stretch ratios of null, 1 × 1, 2 × 2, and 3 × 3, respectively. The biaxial stretch ratio of 3 × 3 improved the OTR performance of PET/clay composite by approximately 18% compared with that of the unstretched PET/clay. Regarding the PETG/clay and PET/PETG/clay nanocomposites, the biaxial stretch ratio of 3 × 3 also improved their OTR performance by 45% and 34%, respectively. Notably, there were significant improvements in the OTR values of the amorphous PETG-incorporated PETG/clay and PET/PETG/clay after biaxial stretching of 3 × 3.

The incorporation of 6 phr clay into the PET, PETG, and PET/PETG blend reduced the WVTR values by 21%, 12%, and 12%, respectively, and the clay also reduced the OTR values of these specimens by 20%, 7%, and 12%, respectively, as shown in Figure 1. Furthermore, biaxial stretching with stretch ratio of 3 × 3 reduced the WVTR values of PET, PETG, and PET/PETG by 32%, 35%, and 35%, respectively, and it also reduced the OTR values of these specimens by 18%, 45%, and 34%, respectively. As stated previously, biaxial stretch can increase the crystallinity of the PETG/clay from null for the unstretched specimen to 9.40% for specimen of stretch ratio of 3 × 3. The strain-induced crystallization in the PETG polymer might be responsible for the significant improvements of WVTR and OTR properties. However, incorporating PETG has slightly lower effect on the WVTR performance of PET/PETG/clay nanocomposites as compared to the OTR performance. Because both PET and PETG are hydrophobic polymers; hence, strain-induced crystallization minimally changes the WVTR property.

As stated previously, the stretching process made the tactoids smaller and with higher aspect ratios.[18] Based on this result, we schematized the transmission path of gas or water vapor molecules in the PET and PET/PETG matrices, as shown in Scheme 2. In the PET/PETG/clay nanocomposite with smaller and higher aspect-ratio tactoids (i.e., the biaxial stretched specimen), the transmission path was more tortuous than in the unstretched specimen. Accordingly, the highly tortuous transmission path significantly improved the barrier properties of the PET/clay, PETG/clay, and PET/PETG/clay nanocomposites.

CONCLUSION

The PET/clay, PETG/clay, and PET/PETG/clay films were subjected to biaxial stretching with stretch ratios of 1 × 1, 2 × 2, and 3 × 3. Tensile modulus and strength and elongation at break of the biaxially stretched films increased with increasing stretch ratios. The biaxial stretching process improved the dispersion of clay platelets in the PET, PETG, and PET/PETG matrices, decreasing the domain size, increasing the aspect ratios of the platelets, and making the platelets more oriented. The biaxial stretching process also triggered a strain-induced crystallization, increasing the crystallinity of crystalline PET and inducing an aggregation of the amorphous PETG molecules to crystallize. The biaxial stretching process also improved the total light transmittance and haze of the PET/clay, PETG/clay, and PET/PETG/clay films. Similar to other nanocomposite materials, PET/clay, PETG/clay, and PET/PETG/clay films improved the barrier properties of gas and water vapor, and the values of OTR and WVTR decreased with increasing stretch ratios.

ACKNOWLEDGMENTS

The authors gratefully acknowledge the sponsorship from National Science Council of Taiwan, ROC, under the project no. NSC 102-2622-E-168-005-CC3.

REFERENCES

1. Choi, W. J.; Kim, H. J.; Yoon, K. H.; Kwon, O. H.; Hwang, C. I. *J. Appl. Polym. Sci.* **2006**, *100*, 4875.

2. Kim, S. H.; Kim, S. C. *J. Appl. Polym. Sci.* **2007**, *103*, 1262.
3. Chen, H.; Pyda, M.; Cebe, P. *Thermochim. Acta* **2009**, *492*, 61.
4. Je'ol, S.; Fenouillot, F.; Rousseau, A.; Masenelli-Varlot, K.; Gauthier, C.; Briois, J. F. *Macromolecules* **2007**, *40*, 3229.
5. Wu, J. H.; Yen, M. S.; Kuo, M. C.; Wu, C. P.; Leu, M. T.; Li, C. H.; Tsai, F. K. *J. Appl. Polym. Sci.* **2013**, *128*, 487.
6. Wu, J. H.; Yen, M. S.; Kuo, M. C.; Wu, C. P.; Leu, M. T. *J. Appl. Polym. Sci.* **2014**, *131*, 39869.
7. Liu, R. Y.; Schiraldi, D. A.; Hiltner, A.; Baer, E. *J. Polym. Sci. Part B: Polym. Phys.* **2002**, *40*, 862.
8. Turner, S. R. *J. Polym. Sci. Part A: Polym. Chem.* **2004**, *42*, 5847.
9. Tsai, Y.; Fan, C. H.; Hung, C. Y.; Tsai, F. Y. *J. Appl. Polym. Sci.* **2007**, *104*, 279.
10. Tsai, Y.; Fan, C. H.; Hung, C. Y.; Tsai, F. Y. *J. Appl. Polym. Sci.* **2008**, *109*, 2598.
11. Papadopoulou, C. P.; Kalfoglou, N. K. *Polymer* **1997**, *38*, 631.
12. Fan, G.; Di Maio, L.; Incarnato, L.; Scarfato, P.; Acierno, D. *Packag. Technol. Sci.* **2000**, *13*, 123.
13. Perrin-Sarazin, F.; Ton-That, M. T.; Bureau, M. N.; Denault, J. *Polymer* **2005**, *46*, 11624.
14. Morgan, A. B.; Gilman, J. W. *J. Appl. Polym. Sci.* **2003**, *87*, 1329.
15. Wu, J. H.; Yen, M. S.; Wu, C. P.; Li, C. H.; Kuo, M. C. *J. Polym. Environ.* **2013**, *21*, 303.
16. Tsai, Y.; Jheng, L.; Hung, C. Y. *Polym. Degrad. Stab.* **2010**, *95*, 72.
17. Zhang, X.; Ajji, A. *J. Appl. Polym. Sci.* **2003**, *89*, 487.
18. Rajeev, R. S.; Harkin-Jones, E.; Soon, K.; McNally, T.; Menary, G.; Armstrong, C. G.; Martin, P. J. *Eur. Polym. J.* **2009**, *45*, 332.
19. Cakmak, M.; Taniguchi, A. *Polymer* **2004**, *45*, 6647.
20. Ajji, A.; Guevremont, J.; Cole, K. C.; Dumoulin, M. M. *Polymer* **1996**, *37*, 3707.
21. Kattan, M.; Dargent, J.; Ledru, J.; Grenet, J. *J. Appl. Polym. Sci.* **2001**, *81*, 3405.
22. Lin, Y. J.; Dias, P.; Chum, S.; Hiltner, A.; Baer, E. *Soc. Plast. Eng.* **2007**, *47*, 1658.